



## Modeling of riparian vegetation dynamics and its application to sand-bed river

Yuji TODA<sup>a,\*</sup>, Yuexia ZHOU<sup>a</sup>, and Norichika SAKAI<sup>b</sup>

<sup>a</sup> Graduate School of Engineering, Nagoya University, Furo-cho, Chikusa-ku, Nagoya 464-8603, Japan

<sup>b</sup> CTI Engineering Co., Ltd., Japan

### ARTICLE INFO

#### Keywords:

Riparian vegetation  
Recruitment  
Growth and expansion  
Destruction  
Bar morphology

### ABSTRACT

A riparian vegetation dynamics model was proposed to consider the mutual influence of hydro-morphology and vegetation dynamics in a sand-bed river. The simulation model consists of four sub-models: river flow and sediment transport, recruitment, growth and expansion, and destruction of vegetation. The numerical simulation was applied to the downstream part of a sand-bed river for predicting the vegetation dynamics over a long period. The model performance is validated by comparison with the field investigation results obtained from analysis of aerial photographs. The simulation results showed that the growth of vegetation starts from the shoreline and the downstream part of sandbars, and the riparian vegetation increases the stability and the relative elevation of the bars. From the good agreements of the temporal tendencies of vegetation recruitment, expansion, and destruction with those obtained from the aerial photographs analysis, the vegetation dynamics model proposed in this study was verified to reproduce the long-term trend of riparian vegetation dynamics fairly well. Finally, the model was applied to different sandbar modes, i.e., alternating bars and multiple bars. The simulation results indicated that the expansion and destruction rates of vegetation show similar tendencies for both bar mode cases, and they were mainly determined by the magnitude of the annual maximum flood. However, the amount of vegetation coverage rate in the alternating bar case was higher than that in the multiple bar case.

### 1. Introduction

The expansion of vegetation on floodplains and main river channels has become a serious problem in East Asian rivers (Asaeda et al., 2015). The expansion of vegetation brings a much larger drag force against river flow, resulting in lower flow velocity and higher water surface level during

floods (Tsujimoto, 1999; Wu, 2005), which can make flood management more difficult. The vegetation increases the stability of a sandbar or floodplain by interrupting the transport of sediment or promoting the deposition of fine sediment (Shimizu et al., 1999). The expansion of exotic vegetation often competes with native species for nutrients, light, and space, and then it may threaten the survival of native species (Darby et al., 1995). Therefore, the dynamics of vegetation not only affects flood management but also the balance of the riparian ecosystem (Hupp, 1991; Darby, 1999), and it is necessary to understand the process and influencing factors on the dynamics of riparian vegetation.

\* Corresponding author:

E-mail address: ytoda@cc.nagoya-u.ac.jp (Y. Toda)

The dynamics of vegetation is easily affected by the river flow regime and river geo-morphological variables (Corenblit et al., 2007) because it develops along the river bank (Naiman, 1997; Greet, 2011), and it always experiences the processes of recruitment, growth and expansion, or destruction over its life cycle. The recruitment of vegetation was pointed out to have the stages of seed dispersal, seed germination, and seedling settlement (Bradley et al., 1986). Hydrochory (water dispersal) was thought to be the dominant dispersal method for riparian vegetation on a river bank (Nilsson et al., 2010). The number of seeds presents an obvious gradual decrease from the shoreline to the upland area of a sandbar because the high frequency of inundation at the shoreline may settle high numbers of seeds there (Fraaije, 2017; Pettit, 2001). The seedling settlement on bare areas may be influenced by the disturbance of drought stress or flooding (Mahoney, 1998; Lytle, 2004). Water table depth was pointed out as a dominant factor for the growth of vegetation (Ridolfi et al., 2006). The destruction of vegetation has been thought to be caused by the duration and magnitude of flooding (Naiman, 1997; Tealdi, 2011) or high-speed water flow (Ye, 2013). The vegetation along a river bank may be washed out by the flow or be buried by sediment deposition during floods.

From the above studies, it can be found that vegetation dynamics has a significant influence on river flow and morphology, and vice versa. The development of vegetation is strongly dependent on hydro-morphological variables, e.g., inundation frequency, water level, and flood magnitude. It means that the relationship between hydrology, morphology, and vegetation dynamics is a mutually influencing process (Tsujimoto, 1999; Camporeale, 2013). Therefore, the development of a numerical simulation model that considers both hydro-morphological variables and vegetation biological variables is required and meaningful for better river management.

Models to simulate the dynamics of vegetation have been proposed in many previous studies. Seed dispersal has been modeled by the seed dispersal distance (Higgins et al., 1999) or the inundation frequency and species tolerance (Auble et al., 1998). The germination of riparian vegetation was pointed out as the function of seed deposition and the consecutive number of days that a plot is not inundated (Dixon et al., 2006). The settlement of riparian vegetation has been modeled as a function of scouring of the river bed and inundation (Dixon et al., 2006). The growth of vegetation has been calculated by the growth rate and diameter of vegetation (Botkin, 1972; Shugart, 1977). The destruction of vegetation was modeled as the function of elevations of water stage and topography (Camporeale et al., 2006). The above studies mainly focused on the specific stages of vegetation dynamics. However, from the viewpoint of river management, the prediction model of vegetation dynamics over a long period, e.g., 10 years and

more, is more significant. The main objective of this study is to explore the dynamics of vegetation over a long period with consideration of the vegetation development processes, e.g., recruitment, growth, and destruction, and the physical characteristics of the river, e.g., discharge, sediment size, river slope, and width of the main channel. The relationship between the dynamics of vegetation and the macro features of a river has been examined in a previous study (Toda et al., 2012a), which mainly focused on field data analysis, such as vegetation distribution and flow regime over a long period, using aerial photographs.

In this study, a vegetation dynamics model is proposed for simulating the long-term alteration of riparian vegetation. First, aerial photography analysis was conducted to identify actual changes in riparian vegetation in the target site. Second, the vegetation dynamics model was established. As the period of the present simulation is long-term, ranging around 20 years, the biological activities of vegetation, such as recruitment, competition, growth, and expansion, were considered in this model. Third, the vegetation dynamics measured by aerial photographs and the simulation results were compared for validation of the proposed model. Finally, the vegetation dynamics model was applied to different sandbar modes to identify the effect of river morphology on the vegetation dynamics.

## 2. Materials and method

### 2.1 Target study site

A sand-bed river, the Yahagi River, is selected as the target river for validation and application of the proposed model. The total length of its main river channel is around 117 km, and its basin area is 1,830 km<sup>2</sup>. Seven dams were constructed at the Yahagi River at the around from 34.0 km to 80.0 km upstream from the river mouth, and the river bed tends to be stable with the construction of dams. The development of sandbar is obvious at the downstream of the Yahagi River, and the alternating bar and multiple bar was formed at the area with narrow and wide river width, respectively. The rapid expansion of riparian vegetation has been reported with the stability of river bed, and it has become a serious problem at the Yahagi River.

The study target site for the investigation of vegetation distribution is located at around 30 km from the river mouth. **Figs. 1(a)-(c)** show aerial photographs of vegetation in this segment. In 1974 and 1987, bare area was the dominant land cover type, and woody vegetation (trees) was found only along the levees of the river. The recruitment expansion of grass was identified at the shoreline and sandbar from 1974 to 1987. The recruitment and expansion of trees on sandbars were easily identified from 1987 to 2007, and it was mainly distributed along the shoreline and the downstream part of sandbars. The predominant types of

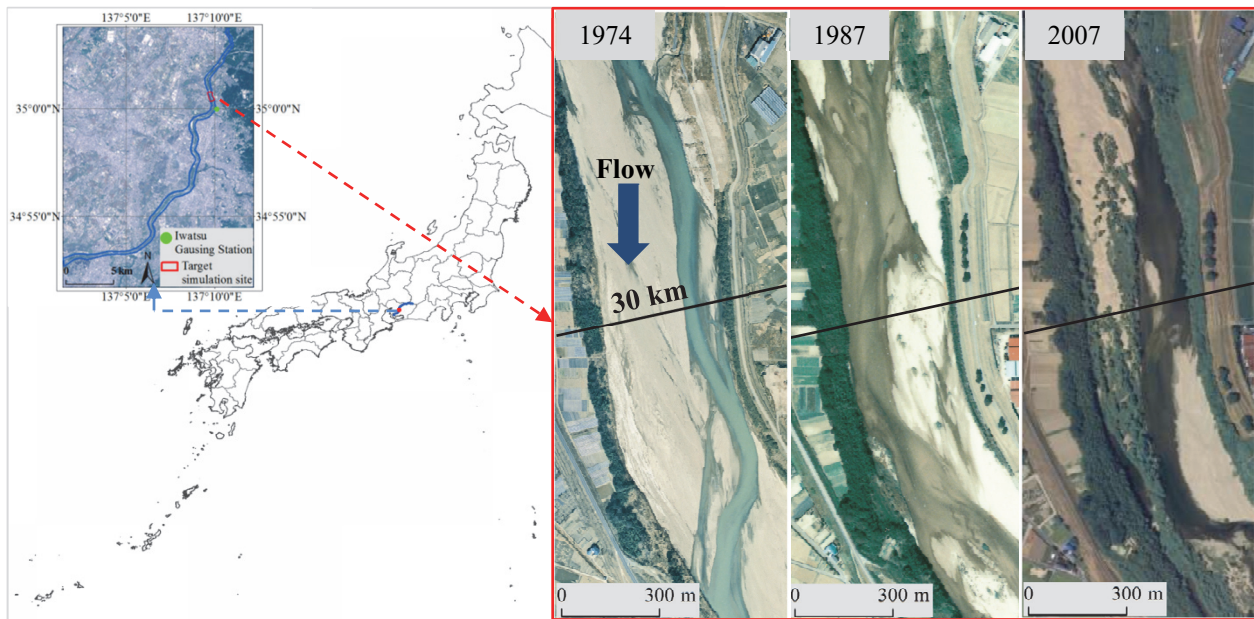


**Fig. 1** Location of the study site and land cover changes at this site

grasses and trees at this study site are *Phragmites japonica* and *Salix subfragilis*, respectively, with heights of 1~2 and 5~10 m.

## 2.2 Aerial photographs analysis

The spatial distribution of riparian vegetation at the study site was identified by aerial photographs analysis, in which aerial photographs taken in 1964, 1974, 1976, 1979, 1985, 1987, and 1992 were used. ArcGIS was used for the analysis, and the specific procedures are as follows:

First, maximum likelihood classification (MLC) was used for the classification of the land cover by referring to the brightness and color composition of the photographs. The land cover of the study site was classified into zones of tree, grass, bare bar, and water. Because the RGB codes of sandbars with shallow water and tree zones were similar, it is difficult to accurately classify sandbars and tree zones using MLC. Therefore, edge detection was then used to further classify zones with similar colors. The error rate of the land cover classification was limited within 5% by the combination of MLC and edge detection image analysis. Then, artificial areas, such as cultivation and parking area, were classified by visual estimation. Finally, the land cover of the main river channel at the study site was classified into five patterns, i.e., grass area, tree area, water area, bare bar area, and artificial area.

The areas of vegetation recruitment and destruction were judged by comparing the change in land cover from the previous year. The rate of vegetation cover, recruitment, and destruction was calculated by the proportion of the vegetation cover area, recruitment area, and destruction area

to the main river channel area, respectively.

## 2.3 Vegetation dynamics model

The proposed vegetation dynamics model is divided into two main parts, i.e., ordinary period and flood period. The initial river morphology, sediment diameter, discharge, and distribution of vegetation are used for the input data of the simulation. In the flood period, the hydro-morphological variables (flow velocity, water depth, sediment transport, and resulting river bed morphology) and the destruction of riparian vegetation are simulated. In the ordinary period, the growth, expansion, and interspecific competition of riparian vegetation are calculated. The simulation of vegetation recruitment is conditional, which is explained in detail in Section 2.3.2. The flowchart of the numerical simulation is shown as **Fig. 2**.

### 2.3.1 Flow and sediment transport

The depth-averaged flow velocity, water depth, and bottom shear stress are simulated by employing the depth-averaged continuity equation and momentum equations under the curvilinear coordinates (Hirakawa et al., 2012). The influence of riparian vegetation on flow is included in the momentum equations by a form drag formula, which considered the density of vegetation (Toda et al., 2005). As for the sediment transport and river morphodynamics during the flood period, the effect of suspended load is neglected, and only the bed load transport is considered for the evolution of the river bed. The MPM equation (Meyer-peter and Müller, 1948) and Hasegawa equation (Hasegawa, 1981) are used for the calculation of bed load transport in the longitudinal and lateral directions,

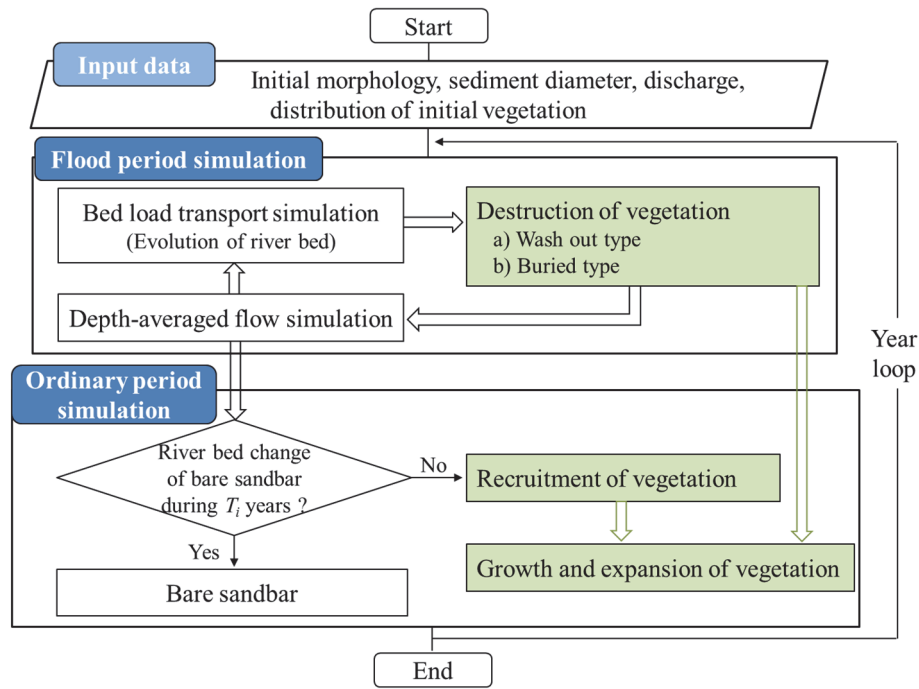


Fig. 2 Flowchart for the vegetation dynamics model

respectively. To simplify the simulation model, flooding is assumed to happen only once per year, and the other periods are regarded as ordinary flow periods.

### 2.3.2 Recruitment of vegetation

The recruitment of vegetation is strongly affected by the biological strategies of seed dispersal (Gurnell et al., 2006), and it was reported that soil seeds along a shoreline are mainly dispersed by river flow (Nilsson et al., 2010). In the present vegetation recruitment model, seeds are assumed to be settled by flowing water dispersal between the relative elevation of the water surface level of the maximum discharge in seed dispersal season ( $z_0$ ) and the ordinary flow shown in Fig. 3. Haslam (1972) pointed out that *Phragmites*, the predominant vegetation type in the study site, release their seeds (wrapped in fruit) during winter and spring. The seeds deposited during winter determined the highest species richness when high river flow can disperse seeds effectively from upstream (Gurnell, 2006; Moggridge, 2009). By referencing the previous studies, the period of the seed dispersal season is assumed to be from December to March in this simulation. The maximum discharge in the seed dispersal season and the ordinary flow discharge are evaluated from the observed discharge data for every year; therefore, the vegetation recruitment area varies every year. The ordinary flow discharge is determined to be the discharge below which the daily maximum discharge does not fall for 185 days in the year. Since disturbance of bare areas by flooding interferes with the settlement of riparian

vegetation (Mahoney, 1998; Lytle, 2004), the recruitment of vegetation at any given point is assumed to be successful if the river bed elevation of this point has not changed during  $T_i$  years (Yagisawa et al., 2009), in which the subscript “ $i$ ” denotes the index for grass ( $g$ ) or tree ( $t$ ). In this study, the duration of the settlement (successful recruitment) of vegetation is assumed as  $T_g = 2$  years for grass and  $T_t = 5$  years for trees by considering the actual change of vegetation observed in the aerial photographs to identify the predominant vegetation specie at the study site.

Compared with the upland of a sandbar, the shoreline of a bar may experience a higher frequency of inundation, which then induces a higher density of soil seeds along the shoreline (Fraaije, 2017) and promotes relatively greater biomass. The rate of the recruitment of vegetation has not been clarified enough, and the trend is different in each river. To apply this model easily to different rivers, the recruitment of riparian vegetation is represented by giving an initial biomass evaluated by considering the frequency of submergence: the initial biomass is larger in the area closer to the shoreline, and the initial biomass is smaller in the area with relative higher elevation, which are modeled by the following relation:

$$M_i = \frac{z_0 - z}{z_0} M_{i0} + M_{i0\min}, \quad (1)$$

where  $z_0$  is the relative height of the water surface level at the maximum discharge during seeds dispersal season with respect to the ordinary water surface level,  $z$  is the relative

height from the ordinary water surface level,  $M_{i0}$  is the initial biomass at the water edge, and  $M_{i0min}$  is the initial biomass when the inundation frequency equals 0 during the seed dispersal period. These values mentioned above strongly affect vegetation dynamics, and further studies on this subject are necessary.

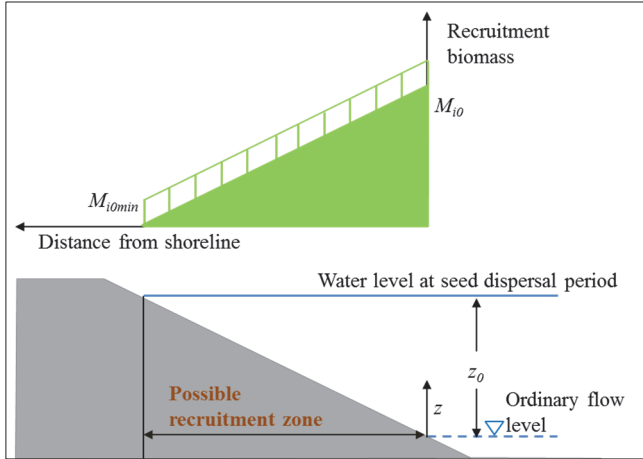


Fig. 3 Modeling of vegetation recruitment to bare sandbar

### 2.3.3 Growth and expansion of vegetation

The growth of vegetation is estimated by the balance between primary production and respiration (Boysen-Jensen, 1932). The competition between vegetation species and the horizontal expansion of vegetation were considered at the riparian vegetation growth period. The interspecific competition among the vegetation species was mainly caused by the need to acquire the solar light necessary for photosynthesis. The higher vegetation is considered to assimilate more light for conducting photosynthesis. The expansion of vegetation in the horizontal direction is calculated in the vegetation growth equation with the format of a diffusion formula.

The change of grass and tree biomass per unit time is calculated as the function of vegetation net growth and the horizontal expansion of surrounding vegetation as follows:

$$\frac{\partial M_i}{\partial t} = P_i - R_i + \frac{\partial}{\partial x} \left( k_{xi} \frac{\partial M_i}{\partial x} \right) + \frac{\partial}{\partial y} \left( k_{yi} \frac{\partial M_i}{\partial y} \right), \quad (2)$$

where  $M_i$  is the biomass per unit area;  $P_i$  is the production by photosynthesis;  $R_i$  is the metabolic rate by respiration; and  $k_{xi}$  and  $k_{yi}$  are diffusion coefficients in  $x$  and  $y$  directions, respectively. The subscript  $i$  ( $=g, t$ ) shows two types of vegetation, i.e., grass ( $g$ ) and tree ( $t$ ).

The Monod function (Tamiya, 1951) is given by formula (3), which was employed for calculating the photosynthesis rate of vegetation per unit of height.

$$p_i = \frac{I}{I + I_{ci}} p_{maxi}, \quad (3)$$

where  $p_i$  is the photosynthesis rate per unit height,  $I$  is illuminance of the vegetation height of  $z$ ,  $I_{ci}$  is the half saturation constant of illuminance, and  $p_{maxi}$  is maximum photosynthesis rate.

The vertical decrease of illuminance in the vegetation canopy is given by the following formula (Monsi and Saeki, 1953):

$$\frac{\partial I}{\partial z} = -\lambda I, \quad (4)$$

where  $\lambda$  is the extinction coefficient of solar light defined as

$$\lambda = \sum_i k_i F_{ci}, \quad (5)$$

where  $F_{ci}$  is the accumulated leaf area index and  $k_i$  is the extinction coefficient per unit leaf area index for each type of vegetation.

By using these equations, the amount of production by photosynthesis per unit area,  $P_i$ , is calculated by integrating the photosynthesis rate per unit volume from the height of vegetation to ground level:

$$P_i = \int_0^{l_i} p_i dz, \quad (6)$$

where  $l_i$  is the height of vegetation.

In this simulation, the proportion of each plant organ to the overall vegetation body is assumed to be constant, and the proportion of each plant organ biomass to the overall riparian vegetation biomass is defined as  $l_{li}$  (leaf),  $l_{si}$  (stem), and  $l_{ri}$  (root). Grass type vegetation is assumed to have the organs leaf and root, with organ biomass proportions of 0.1 and 0.9, respectively. Tree type vegetation is assumed to have the organs root, stem, and leaf, with organ biomass proportions of 0.3, 0.2, and 0.5, respectively. The height of vegetation above the ground is calculated as formula (7) by utilizing the proportions defined above:

$$l_i = \frac{(l_{li} + l_{si}) M_i}{\rho_i A_i}, \quad (7)$$

where  $\rho_i$  is the specific weight of vegetation and  $A_i$  is the cross-sectional area density of vegetation.

The metabolic rate by respiration is given by the sum of amounts of respiration needed for growth and maintenance, proposed by McCree (1970) as follows:

$$R_i = \gamma_i P_i + \mu_i M_i, \quad (8)$$

where  $\gamma_i$  is the coefficient of respiration for growth and  $\mu_i$  is the coefficient of respiration for maintenance.

### 2.3.4 Destruction of vegetation

Naiman (1997) and Tealdi (2011) have pointed out that flood duration and magnitude are the dominant factors for the destruction of riparian vegetation. In the present model,

the destruction of riparian vegetation is assumed to occur during flood periods. The destruction of grasses and trees is classified into two types based on the evolution of river bed around the vegetation stand. The first type is washing out for the case that the river bed around the riparian vegetation was scoured. The second type is buried for the case that the river bed around the riparian vegetation was elevated. The destruction of the washing out type occurs when either the bottom shear stress acting on the riparian vegetation surpasses the critical washing out shear stress of vegetation  $\tau_c$  (Yagisawa et al., 2009) or the local river bed scour depth caused by flooding becomes larger than the vegetation root depth. The destruction of the buried type is regarded to occur under the following two cases. One case is that the riparian vegetation is completely buried, i.e., the height of sediment deposition is larger than that of the vegetation above the ground, and this is considered to completely destroy the vegetation. Another case is that only part of the vegetation is buried, i.e., the height of sediment deposition is smaller than that of vegetation above the ground. In this case, the decreased vegetation biomass is estimated to be proportional to the buried height of vegetation.

### 3. Computational condition

To validate the effectiveness of the proposed vegetation dynamics model, the dynamics of vegetation and geo-morphology in the target river during around 20 years (1971 to 1992) were simulated. In the flow and sediment transport simulation, the average river bed slope is set to be 1/1,000 and the sediment diameter is represented by the uniform value of 5 mm. A compound cross-section is used for the initial river morphology condition, and the cross-section of the river channel at a location 30 km from the Yahagi River mouth was simplified into a line-shaped compound channel section (red line in Fig. 4). In this condition, alternating sandbars were generated in the main channel with a wave length around 1.5 km and wave height around 2.0~2.4 m, which is similar to the scale of sandbars at the target study site. The river bed evolution of flood plains is not considered in this simulation model, and the sediment transport and the resulting river bed evolution are only considered in the main channel.

The discharge for the ordinary period is set as the constant value of 30 m<sup>3</sup>/s, because the discharge at the study site was controlled by the upstream dams with the record of around 30 m<sup>3</sup>/s. The input hydrograph for the flood period is set from the calculation of the actual annual maximum discharge (validation interval in Fig. 5) obtained from the Iwatsu discharge gauging station (Fig. 1), which is located at 29.24 km upstream from river mouth, during 1971 and 1992. The calculation of the hydrograph in the flood period is shown as formula (9).

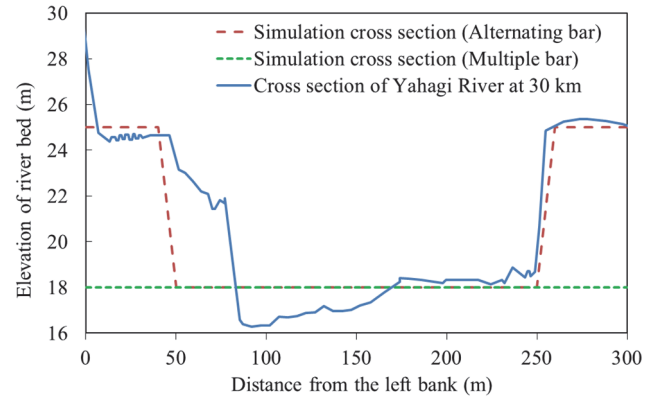


Fig. 4 Cross-section of the study site and simulation

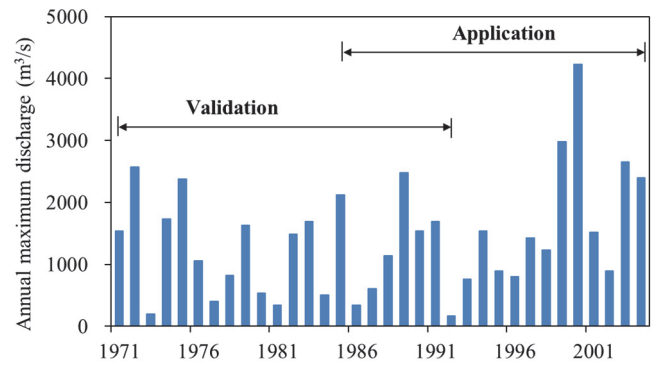


Fig. 5 Annual maximum discharge used in the simulation

Table 1. Vegetation parameters used in the simulation

Parameter	Grass	Tree	Reference
$A_i$ (cm <sup>2</sup> / cm <sup>2</sup> )	1	1	Assumed
$\rho_i$	1.5	1.5	Assumed
$p_{maxi}$ (g/cm·day)	0.23	$3.4 \times 10^{-2}$	Kira,1969
$F_{ci}$ (cm <sup>2</sup> /cm)	0.028	$3.3 \times 10^{-3}$	Jensen,1932
$I_{ci}$ (lx)	4,000	500	Kira,1969
$k_i$	0.5	3.0	Kira,1969
$\gamma_i$	0.25	0.05	Hesketh,1971
$\mu_i$	0.05	0.01	Hesketh,1971
$k_{xi}, k_{yi}$	4.0	2.0	Observed
$\tau_{ci}$ (N/m <sup>2</sup> )	120	67	Yagisawa,2009
$M_{i0}$ (g/cm <sup>3</sup> )	114.0	114.0	Assumed
$M_{i0min}$ (g/cm <sup>3</sup> )	6.0	6.0	Assumed

$$Q(t) = (Q_p - Q_0) \sin^2\left(\frac{t-t_0}{T} \pi\right) + Q_0 \quad (9)$$

where  $Q_p$  is the peak daily discharge during one year,  $Q_0$  is the ordinary discharge,  $t_0$  is the start time of flooding, and  $T$  is the flood duration. Here, the flood duration is set as 40 hours by referring to the monitoring flooding period at the Iwatsu gauging station.

In the simulation, *Phragmites japonica* and *Salix subfragilis* are the predominant types of grass and tree, respectively. The vegetation parameters are summarized in **Table 1**. The seasonal difference of illuminance was not considered in the present model, and it is assumed as the constant value of 9,500 lx. The initial biomass of vegetation on the sandbar is assumed to be zero.

## 4. Results and discussion

### 4.1 Validation of the model

#### 4.1.1 Spatio-temporal development of vegetation and bar morphology

**Figs. 6(a)-(d)** present the simulation results of the spatio-temporal distribution of the biomass of grasses and trees, and the elevation of the bar bed in 1975, 1977, 1982, and 1987, respectively. From **Fig. 6(a)**, we can find that the grass recruitment zones are mainly distributed at the downstream part of sandbars, where the flow velocity and bottom shear stress are smaller than that on the upstream part of the bar. Therefore, the prior invasion of riparian vegetation was promoted on the downstream side of bars.

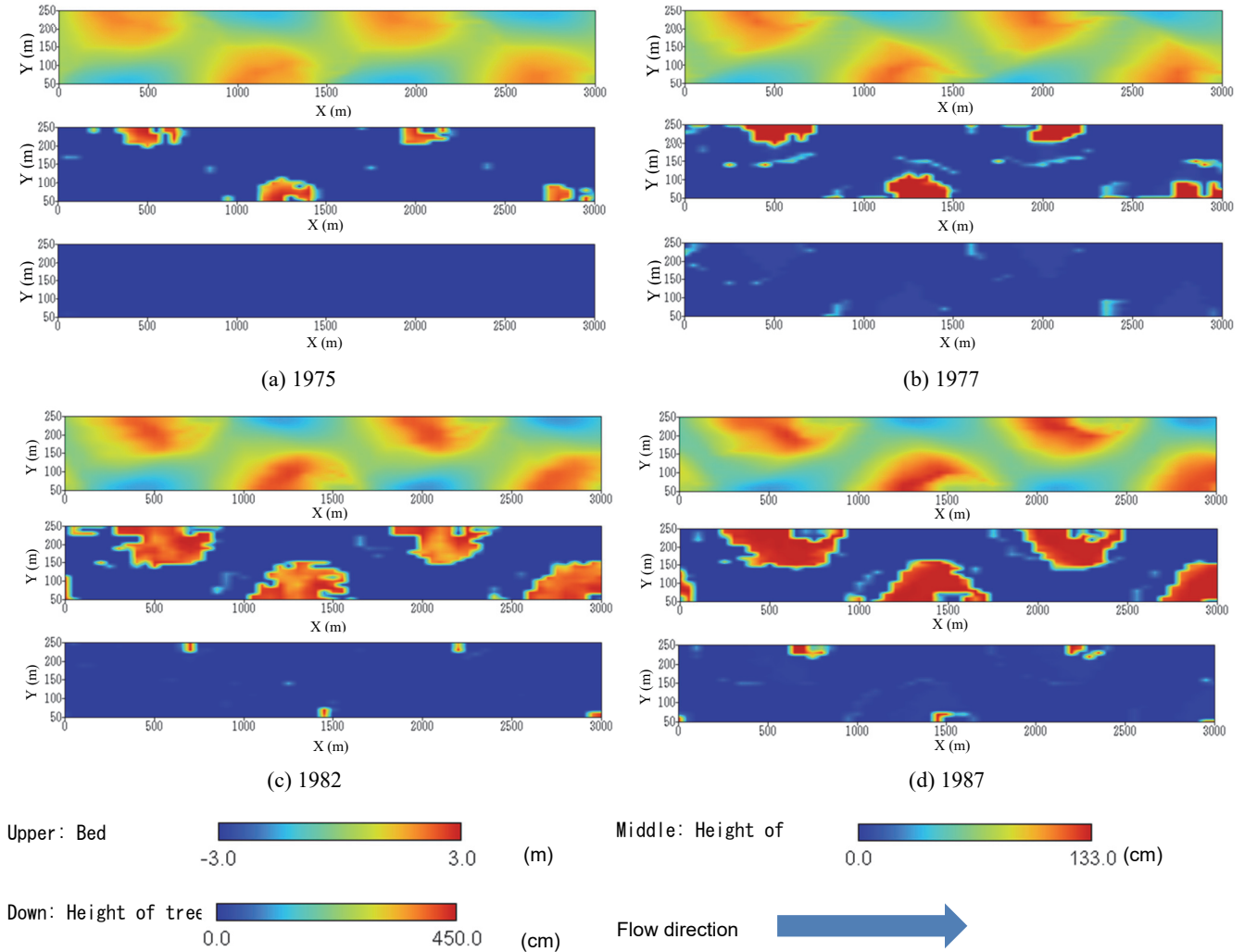


**Fig. 6** Spatio-temporal evolution of sandbar morphodynamics and development of vegetation height

From **Figs. 6(b)-(d)**, it was found that the vegetation recruitment area distributed along the shoreline of the bars with an almost linear shape, which is a common

phenomenon seen in the investigation of actual rivers [**Fig.1(c)**; Zhou et al., 2018]. The distribution of the riparian vegetation recruitment zone along shoreline with linear

shape may be explained from the following aspects. With reference to the seed dispersal strategy along a river bank, the recruitment biomass is abundant at the shoreline zone where  $z=0$  (Fig. 3); however, it is vulnerable to be destroyed during floods. At the same time, the recruitment biomass at the zone of  $z=z_0$  is scant (Fig. 3), and it is also much easier to be destroyed by drought pressure during ordinary flow periods. Therefore, it is difficult for the initial recruitment vegetation to survive in these two zones. In contrast, the recruitment vegetation located in the zone where  $0 < z < z_0$  (Fig. 3) may “escape” from the destruction of floods, and achieve final “success” with the formation of a linear shape along the shoreline of the bar. From the above analysis, it can be found that the proposed vegetation recruitment model can reproduce the initial riparian vegetation recruitment in a sand-bed river.

From the graph of bed evolution in Figs. 6(a)-(d), it can be seen that the sandbar was almost stabilized. The relative elevation of the bar recruited by the grass and tree progressively increases along the transverse direction from Figs. 6(a)-(d). This may be caused by the trapping of sediment as an effect of vegetation, which decreases the flow velocity and retains sediment transported to the bar. Shimizu et al. (1999) also pointed that the vegetation can interrupt the transport of sediment, which strengthened the stabilization of the river bed. The increasing relative elevation between the water area and bar area reduces the submergence frequency of the sandbar, and this prevents vegetation destruction by flooding, which provides a more stable zone for the further expansion of vegetation. The interactive influence between the stabilization of sandbar and the expansion of vegetation was clearly expressed in the present simulation.

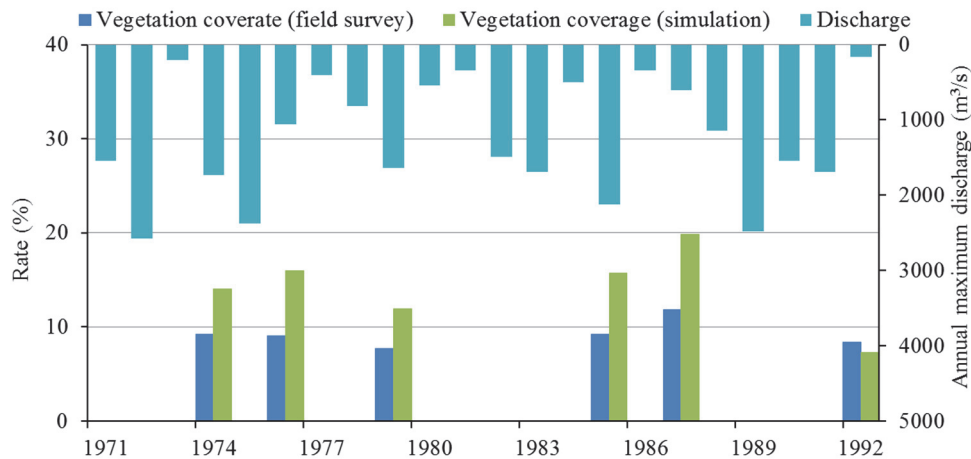
#### 4.1.2 Temporal dynamics of vegetation

Since the cross-section shape of the river was simplified in this simulation, it is difficult to discuss the change of vegetation at the specific point of the study site in detail.

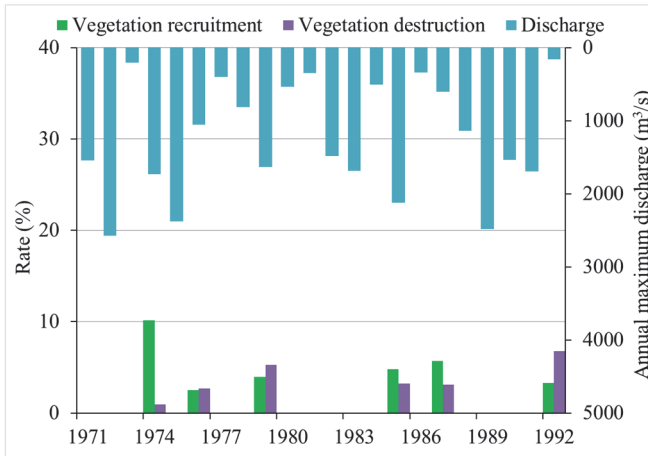
The dynamics of vegetation, e.g., the rates of coverage, recruitment, and destruction over a long period (around 20 years) was analyzed from a comprehensive view based on the changes in vegetation over the whole main river channel. The vegetation dynamics in the investigation results using aerial photographs analysis and the simulation results are shown in Fig. 7.

Figs. 7(a)-(c) present the annual maximum discharge and the temporal change of the rates of vegetation coverage, recruitment and destruction of the results by aerial photograph analysis and numerical simulation, respectively. From the comparison, the rate of vegetation coverage was a little overestimated (Fig. 7(a)). In the present simulation, the rates of vegetation recruitment, which is related to the initial biomass at the water edge, are a litter overestimated, which leads to the overestimation of the rate of vegetation coverage. This indicates that the determination of initial biomass should be further improved in the future. The natural death of plants and thinning was not considered in this vegetation dynamics model, which may also result in the overestimation of the rate of vegetation coverage. But the temporal trends of the vegetation coverage are represented appropriately by the simulation. Furthermore, Figs. 7 (b) and (c) show that the relative magnitudes of the vegetation destruction and recruitment rates in the simulation are almost the same with the measured results. Therefore, the present model can reproduce the tendency of vegetation expansion or reduction fairly well.

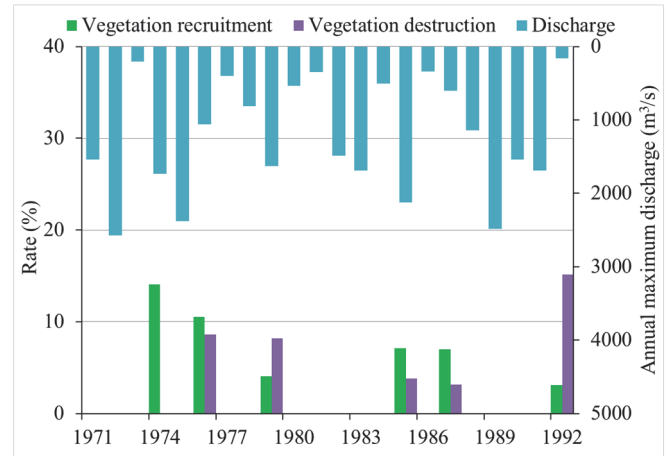
From the above discussions, the present simulation model can be regarded as representing the interaction between bar morphodynamics and riparian vegetation dynamics, as well as expressing the temporal trends of vegetation dynamics over a long period. Therefore, the present proposed vegetation dynamics model was applied to different sandbar modes to identify the effect of bar mode on the dynamics of vegetation for another long period from 1985 to 2004.



(a) Rates of vegetation coverage of field survey and simulation



(b) Rates of vegetation recruitment and destruction of field survey



(c) Rates of vegetation recruitment and destruction of simulation

**Fig. 7** Comparison of rates of vegetation coverage, recruitment, and destruction

#### 4.2 Application of the model to different bar modes

To identify the effects of bar modes on vegetation dynamics, the present vegetation dynamics model was applied to both alternating bar and multiple bar cases. The computational conditions of the alternating bar case are the same as those of the validation case explained in section 3. The river width of these two modes of bar are same (300 m), however, the main channel for the multiple bar case was set into single channel section (green line in **Fig. 4**). Under these conditions, the multiple bars with around 1 km wave length and about 1.2 m wave height were generated. The other computational conditions are the same with the alternating sandbar stated in section 3.

The input hydrograph in simulation is calculated from the annual maximum discharge between 1985 and 2004 (application interval in **Fig. 5**) based on formula (9). The vegetation parameters used in the application simulation are shown as in **Table 1**, and the initial biomass of vegetation on sandbars is assumed to be zero.

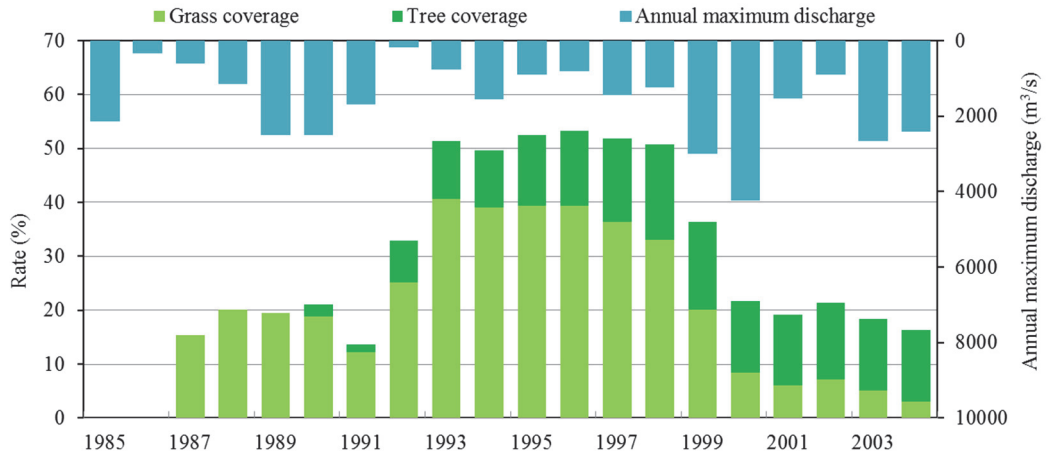
##### 4.2.1 Temporal dynamics of vegetation under different bar modes

**Fig. 8** and **Fig. 9** show that the temporal dynamics of vegetation between 1985 and 2004 for the alternating bar and multiple bar cases, respectively. **Fig. 8(a)** and **Fig. 9(a)** show that the coverage rate of grass almost reached the highest value at 1993 in both bar mode cases. This resulted from the smaller annual maximum discharge during 1992 and 1993, which promoted the stabilization of the sandbar. The immobilization of the sandbar increases the recruitment rate of vegetation and decreases the destruction rate of vegetation. The vegetation coverage rate maintains almost the same high-level status during 1993~1998 due to the relative small floods during these years. The vegetation coverage rate obviously decreases under the effect of large

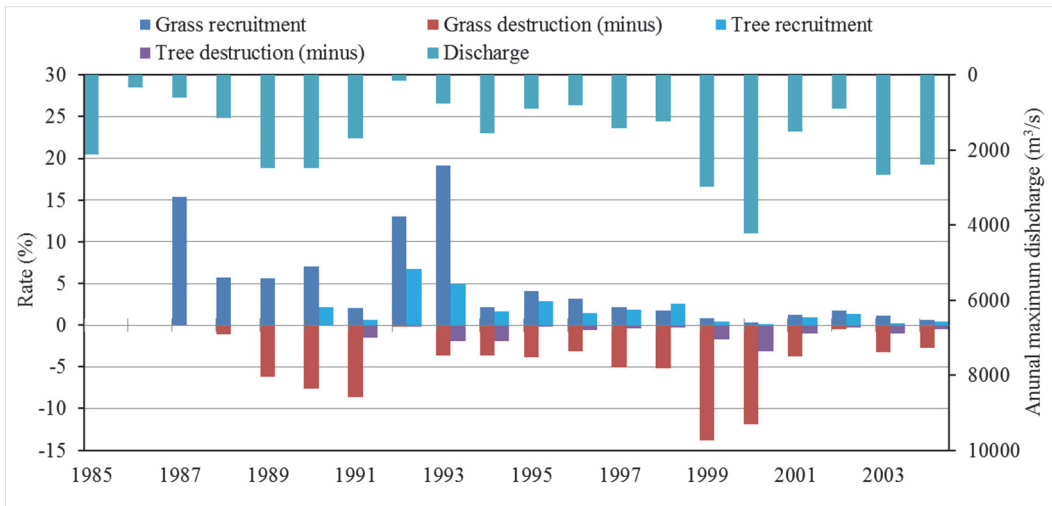
floods in 1999 and 2000, which destabilized the sandbar, resulting in a high destruction rate and low recruitment rate of vegetation. From the simulation results of the two different bar modes, it can be found that the temporal change of vegetation (expansion or reduction) presents the same trend in either alternating or multiple sandbars, and the time trend of vegetation is mainly determined by the magnitude of flooding. In the previous studies, it was also reported that the magnitude of flooding is a critical factor for the dynamics of vegetation (Naiman, 1997; Tealdi, 2011).

Although the time trends are the same, some differences still existed in the different bar morphologies. Comparison of **Fig. 8(a)** and **Fig. 9(a)** shows that a difference in vegetation coverage rate is evident for different bar modes, and the vegetation coverage rate for the alternating bar case is obviously higher than that at the multiple bar case. **Fig. 8(a)** shows that the coverage rate for trees reaches almost 10% in the alternating bar case after 20 years; however, it is only around 1% in the multiple bar case (**Fig. 9(a)**). These comparisons suggest that the sandbar mode is a significant factor for the expansion of vegetation and recruitment of trees in a sand-bed river. Toda et al. (2012b) pointed out that the vegetation dynamics was influenced by the sandbar mode after comparing the vegetation dynamics and sandbar modes in 8 Class-A rivers in the Chubu region of Japan.

**Fig. 8(b)** shows that the grass dynamics (recruitment or destruction) is sensitive to the magnitude of flooding, while the tree destruction rate is almost unresponsive to flooding even under large flood magnitudes. Therefore, the expansion of trees may be irreversible, and it is difficult to destroy them with natural forces once they have widely grown on the sandbar. This means the trees may develop into the dominant vegetation type with the expansion of vegetation, which is identified in the investigation (**Figs. 1(b)** and **(c)**).

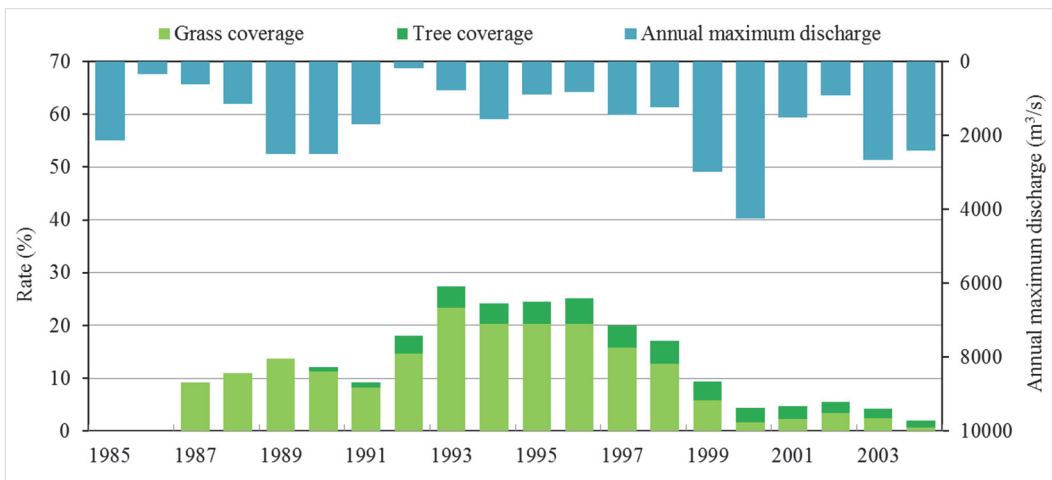


(a) Rates of vegetation coverage

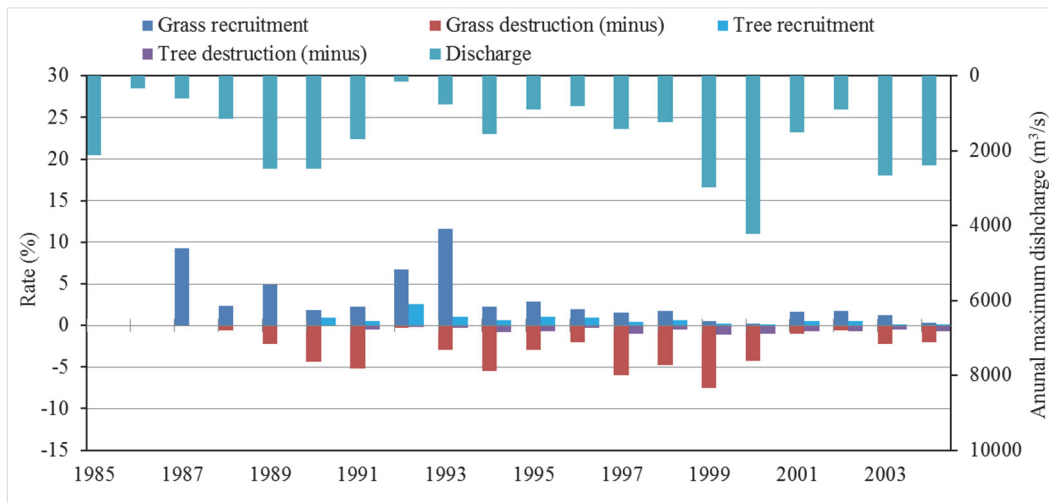


(b) Rates of vegetation recruitment and destruction

**Fig. 8** Temporal dynamics of vegetation for alternating bar



(a) Rates of vegetation coverage



(b) Rates of vegetation recruitment and destruction

**Fig. 9** Temporal dynamics of vegetation for multiple bar

#### 4.3 Limitation of the model

The model proposed in this study was based on the river characteristic of sand bed river, therefore it cannot be effectively applied to the gravel bed river. It was difficult to simulate the multiple and evenly distributed vegetation dynamics by using this model, because only the predominant vegetation type was considered in this study.

In the flood period simulation, the annual maximum discharge and uniform sediment size were considered. The only consideration of annual maximum flood was relative reasonable at some extent in this study, because the moderate and small floods were expected to be controlled or adjusted by the dams constructed at the upstream of the study site. However, as for the no control river, i.e. no hydraulic constructions in the river, the only peak flood used in the simulation is not very accurate. The river bed evolution in the simulation may vary much from the actual condition if there is large difference between the river bed materials in the river.

### 5. Conclusions

In this study, a numerical simulation model that considers the interaction between vegetation dynamics and sandbar morphodynamics was proposed. The vegetation dynamics was modeled under the conditions of the downstream reach of a sand-bed river. The results of the numerical simulation revealed that the proposed simulation model reliably predicts the long-term tendency of riparian vegetation dynamics. The following conclusions can be obtained from the simulation results of the present model:

- Riparian vegetation starts to grow and expand from the downstream part and shoreline of a sandbar.
- The expansion of riparian vegetation increases the

relative height and stabilization of a sandbar, and vice versa. Thus, the stabilization of a bar subsequently promotes the expansion of vegetation.

- The annual maximum flood has an important influence on the time trend of vegetation coverage.
- The sandbar mode is a critical factor for the vegetation coverage rate, which is much larger in the alternating bar case than it is in the multiple bar case.
- The development of tree coverage on a sandbar is almost irreversible because it is difficult to destroy trees with floods.

### References

- Asaeda, T., Rashid, M.H., Abu Bakar, R., 2015. Dynamic modelling of soil nitrogen budget and vegetation colonization in sediment bars of a regulated river. *River Res. Appl.* 31(4), 470-484.
- Botkin, D.B., Janak, J.F., Wallis, J.R., 1972. Some ecological consequences of a computer model of forest growth. *J. Ecol.* 849-872.
- Boysen-Jensen, P., 1932. Die stoffproduktion der pflanzen. Jena.
- Boysen-Jensen, P., 1918. Studies on the production of matter in light and shadow plants. *Bot. Tidsskr.* 36:219.
- Bradley, C.E., Smith, D.G., 1986. Plains cottonwood recruitment and survival on a prairie meandering river floodplain, Milk River, southern Alberta and northern Montana. *Can. J. Bot.* 64(7), 1433-1442.
- Camporeale, C., Perucca, E., Ridolfi, L., Gurnell, A.M., 2013. Modeling the interactions between river morphodynamics and riparian vegetation. *Rev. Geophys.* 51(3), 379-414.
- Camporeale, C., Ridolfi, L., 2006. Riparian vegetation distribution induced by river flow variability: A stochastic approach. *Water Resour. Res.* 42(10), W10415.
- Corenblit, D., Tabacchi, E., Steiger, J., Gurnell, A.M., 2007. Reciprocal interactions and adjustments between fluvial landforms and vegetation dynamics in river corridors: A review of complementary approaches. *Earth-Science Rev.* 84(1), 56-86.

- Darby, S.E., 1999. Effect of riparian vegetation on flow resistance and flood potential. *J. Hydraul. Eng.* 125, 443-454.
- Darby, S.E., Thorne, C.R., 1995. Fluvial maintenance operations in managed alluvial rivers. *Aquat. Conserv. Mar. Freshw. Ecosyst.* 5(1), 37-54.
- Fraaije, R.G.A., Moinier, S., Van Gogh, I., Timmers, R., Van Deelen, J.J., Verhoeven, J.T.A., Soons, M.B., 2017. Spatial patterns of water-dispersed seed deposition along stream riparian gradients. *PLoS One.* 12(9), e0185247
- Greet, J., Angus Webb, J., Cousens, R.D., 2011. The importance of seasonal flow timing for riparian vegetation dynamics: A systematic review using causal criteria analysis. *Freshw. Biol.* 56(7), 1231-1247.
- Gurnell A.M., Boitsidis A.J., Thompson K., Clifford N.J., 2006. Seed bank, seed dispersal and vegetation cover: Colonization along a newly-created river channel. *J. Veg. Sci.* 17(5), 665-674.
- Hasegawa, K., 1981. Bank-erosion discharge based on a non-equilibrium theory. in: *Proceedings of JSCE*, 316, 37-52. (In Japanese)
- Haslam, S.M., 1972. Biological Flora of the British Isles, *Phragmites communis* Trin. *J. Ecol.*, 60, 585-610.
- Hesketh, J.D. Baker, D.N., Duncan, W.G., 1971. Simulation of growth and yield in cotton: Respiration and the carbon balance, *Crop Science.* 11(3), 394-398.
- Hirakawa, R., Watanabe, K., Kominami, T., 2012. Instruction between topographic changes and herbaceous vegetation of sand bar. *JSCE, Ser. A2 (AM).* 68(2), I 617-I 624.
- Hupp, C.R., Simon, A., 1991. Bank accretion and the development of vegetated depositional surfaces along modified alluvial channels. *Geomorphology.* 4, 111-124.
- Kira, T., Shinozaki, K., Hozumi, K., 1969. Structure of forest canopies as related to their primary productivity. *Plant Cell Physiol.* 10(1), 129-142.
- Lytle, D.A., Merritt, D.M., 2004. Hydrologic regimes and riparian forests: A structured population model for cottonwood. *Ecology.* 85(9), 2493-2503.
- Mahoney, J.M., Rood, S.B., 1998. Streamflow requirements for cottonwood seedling recruitment - An integrative model. *Wetlands.* 18(4), 634-645.
- McCree, K.J., 1970. An equation for the rate of respiration of white clover plants grown under controlled conditions, In: *Prediction and Measurement of Photosynthetic Productivity, Proceedings of the IBP/PP Technical Meeting, Trebon, 14-21 September 1969.* 221-229.
- Meyer-Peter, E., Müller, R., 1948. Formulas for bed-load transport, in: *Proceedings of the 2nd Meeting of the International Association for Hydraulic Structures Research.* 39-64.
- Moggridge Helen, L., Gurnell Angela, M., Owen, M.J., 2009. Propagule input, transport and deposition in riparian environments: The importance of connectivity for diversity. *J. Veg. Sci.* 20(3), 465-474.
- Monsi, M., Saeki, T., 1953. Über den Lichtfaktor in den Pflanzengesellschaften und seine Bedeutung für die Stoffproduktion. *Japanese J. Bot.* 14, 22-52.
- Naiman and, R.J., Décamps, H., 1997. The ecology of interfaces: Riparian zones. *Annu. Rev. Ecol. Syst.* 28(1), 621-658.
- Nilsson, C., Brown, R.L., Jansson, R., Merritt, D.M., 2010. The role of hydrochory in structuring riparian and wetland vegetation. *Biol. Rev.* 85(4), 837-858.
- Pettit, N.E., Froend, R.H., 2001. Availability of seed for recruitment of riparian vegetation: A comparison of a tropical and a temperate river ecosystem in Australia. *Aust. J. Bot.* 49(4), 515-528
- Ridolfi, L., D'Odorico, P., Laio, F., 2006. Effect of vegetation-water table feedbacks on the stability and resilience of plant ecosystems. *Water Resour. Res.* 42(1), W01201.
- Shimizu, Y., Kobatake, S., Arafune, T., Okada, S. 1999. Study on the excessive growth of riverine trees in gravel-bed river. *Annual J. Hydraul. Eng., JSCE.* 73, 971-976. (In Japanese)
- Shugart, H., West, D., 1977. Development of an Appalachian deciduous forest succession model and its application to assessment of the impact of the chestnut blight. *J. Environ. Manage.* 5, 161-179.
- Tamiya, H., 1951. Some theoretical notes on the kinetics of algal growth, *Bot. Mag. Tokyo* 64, 163-173.
- Tealdi, S., Camporeale, C., Ridolfi, L., 2011. Modeling the impact of river damming on riparian vegetation. *J. Hydrol.* 396(3), 302-312.
- Toda, Y., Furukawa, T., Tsujimoto, T., 2012a. Development of Aerial photograph analysis for detecting large scale and long term dynamics of riparian vegetation - Case of the downstream segment of the Tenryu River, *Annual J. Hydraul. Eng., JSCE.* 68(4), 739-744. (In Japanese)
- Toda, Y., Furukawa, T. and Tsujimoto, T., 2012b. Comparative study on long term change of riparian vegetation in class-A rivers in Chubu region by using aerial photographs analysis. *Advances in River Eng.* 18, 41-46. (In Japanese)
- Toda, Y., Ikeda, S., Kumagai, K., Asano, T., 2005. Effects of flood flow on flood plain soil and riparian vegetation in a gravel river. *J. Hydraul. Eng.* 131(11), 950-960.
- Tsujimoto, T., 1999. Fluvial processes in streams with vegetation. *J. Hydraul. Res.* 37(6), 789-803.
- Wu, W., Shields, F.D., Bennett, S.J., Wang, S.S.Y., 2005. A depth-averaged two-dimensional model for flow, sediment transport, and bed topography in curved channels with riparian vegetation. *Water Resour. Res.* 41(3), W01015.
- Yagisawa, J., Tanaka, N. 2009. Dynamic growth model of river vegetation considering the destruction by floods and regeneration process of trees, *Annual J. Hydraul. Eng., JSCE.* 53, 1171-1176. (In Japanese)
- Ye, F., Chen, Q., Blanckaert, K., Ma, J., 2013. Riparian vegetation dynamics: Insight provided by a process-based model, a statistical model and field data. *Ecohydrology.* 6(4), 567-585.
- Zhou, Y.X., Kubo, E., Sunahara, K. and Toda, Y., 2018. Distribution and dispersal method of accumulated seeds in upper soil on bare bar in sand bed River. *Annual J. Hydraul. Eng., JSCE.* 74(5), 385-390.